Atmospheric Chemistry Experiment (ACE) satellite observations of aerosols and SO_2 emissions from the 2024 Ruang volcanic eruption

Randika Dodangodage[a,*], Peter F. Bernath[a,b,c], Matthew Wyatt[a], Chris Boone[c]

[a] *Department of Physics, Old Dominion University, Norfolk, VA, United States, 23529*
[b] *Department of Chemistry and Biochemistry, Old Dominion University, Norfolk, VA, United States, 23529*
[c] *Department of Chemistry, University of Waterloo, Waterloo, ON, Canada, N2L 3G1*

Abstract

Indonesia's Ruang volcano erupted on April 16, 2024, with subsequent eruptions on April 17 and 30. The resulting plume was observed rising to altitudes of up to 12 km. **10 days after** the eruption of the Ruang volcano in April 2024, the Atmospheric Chemistry Experiment (ACE) observed notable increases in SO_2 volume mixing ratios and aerosol extinction at an altitude of approximately 20 km. It was confirmed that the aerosols present were sulfate aerosols from their infrared spectra. The composition and size of the stratospheric sulfate aerosol particles were determined by fitting the infrared transmission spectra. The sulfate aerosols observed in the plume were about 64% (by weight) sulfuric acid, and the droplets had an average median radius of 0.127 μm.

Keywords: Ruang volcanic eruption, Atmospheric Chemistry Experiment (ACE), SO_2, Sulfate aerosols

1. Introduction

Volcanic eruptions are powerful natural phenomena that have a profound impact on the chemistry of the Earth's atmosphere and on climate. During an eruption, substantial amounts of ash, sulfur compounds (primarily SO_2), water vapor, and other molecules are released into the atmosphere [1]. Although the amount of water vapor emitted during an eruption is usually small, the 2022 Hunga eruption injected a large quantity of water vapor into the stratosphere [2, 3, 4]. Depending on the magnitude of the eruption, SO_2 can be transported into the stratosphere forming sulfate aerosols, where they **can potentially** significantly alter the chemistry (for example, changing the ozone composition) [5, 6, 7]. Emitted SO_2 rapidly converts to sulfuric acid in the troposphere within a few days, whereas in the stratosphere, this process can take several weeks or months [1]. Stratospheric aerosols scatter incoming solar radiation, leading to surface cooling, and heat the stratosphere by absorbing outgoing thermal radiation. The Pinatubo eruption in 1991 caused a decrease in the Earth's average surface temperature by 0.4 K [8, 9, 10] and led to a 3-4% reduction in stratospheric ozone [11, 12].

The Ruang volcano is situated on the Sangihe volcanic island near the equator (2.3°N, 125.37°E), one of 22 volcanic islands in Indonesia [13]. The volcano erupted on April 16, 2024, and the Darwin Volcanic

*Corresponding author
Email address: rdodango@odu.edu (Randika Dodangodage)

Ash Advisory Center (VAAC) noted an ash plume visible in satellite images rising to 1.2 km above sea level. Later, on 17 April, an ash plume rose to 9.1 km, and another plume reached 12.2 km, detaching from the summit [14].

The Advanced Himawari Imager (AHI) on Japan's Himawari-9 satellite [15] captured the Ruang eruption as it ejected a massive ash and SO_2 plume into the atmosphere [16]. **The Ozone Monitoring Instrument (OMI) [17], combining data from April 17 - 19, observed the SO_2 plume initially moving east. However, as higher altitude (4-19 km) winds took effect, the plume moved west [18]. About ten days later, ACE captured the plume to the west of Ruang.** The Support to Aviation Control Service (SACS), hosted by the Royal Belgian Institute for Space Aeronomy [19], provides near-real-time SO_2 and ash data from various satellite instruments, including Global Ozone Monitoring Experiment (GOME-2) [20], Tropospheric Monitoring Instrument (TROPOMI) [21], Ozone Mapping and Profiler Suite (OMPS) [22], and OMI in the UV/Visible range, as well as Infrared Atmospheric Sounding Interferometer (IASI) [23] and Atmospheric InfraRed Sounder (AIRS) [24] in the infrared. On April 18, 2024, GOME-2, TROPOMI, OMPS, AIRS, and IASI[C] reported **SO_2** vertical column densities of more than 50 DU. TROPOMI and IASI indicated SO_2 plume heights reaching 18 km and above. OMPS data reveal the SO_2 plume extending across 30° and reaching 90°E by April 20. By April 24, these instruments showed that the entire plume had moved west and risen above 18 km. Fig. 1 illustrates the SO_2 plume observed by TROPOMI, OMPS, and IASI, with images sourced from SACS [19]. On April 18, TROPOMI captured the plume, as shown in Figs. 1a and 1b. A secondary eruption occurred on April 30, resulting in at least three eruptive events that produced ash plumes reaching heights of at least 1.5 km [25]. The VAAC reported that these ash plumes detached from the summit and drifted west and southwest. Fig. 1d shows SO_2 plumes from both eruptions, with the plume from the initial eruption drifting west. **Satellite images continued to capture these plumes moving west through early May (Figs. 1e, 1f, 1g, and 1h)**. The Himawari satellite measured a total SO_2 emission of approximately 0.5 Tg on April 17, while other satellites recorded about 0.3 Tg the following day [26]. **During the secondary eruption, the ACE satellite captured measurements near tropical latitudes, detecting injections from the eruption, which were later observed at around 20 km altitude in June, likely originating from the later eruption. Section 2 discusses ACE measurements and locations.**

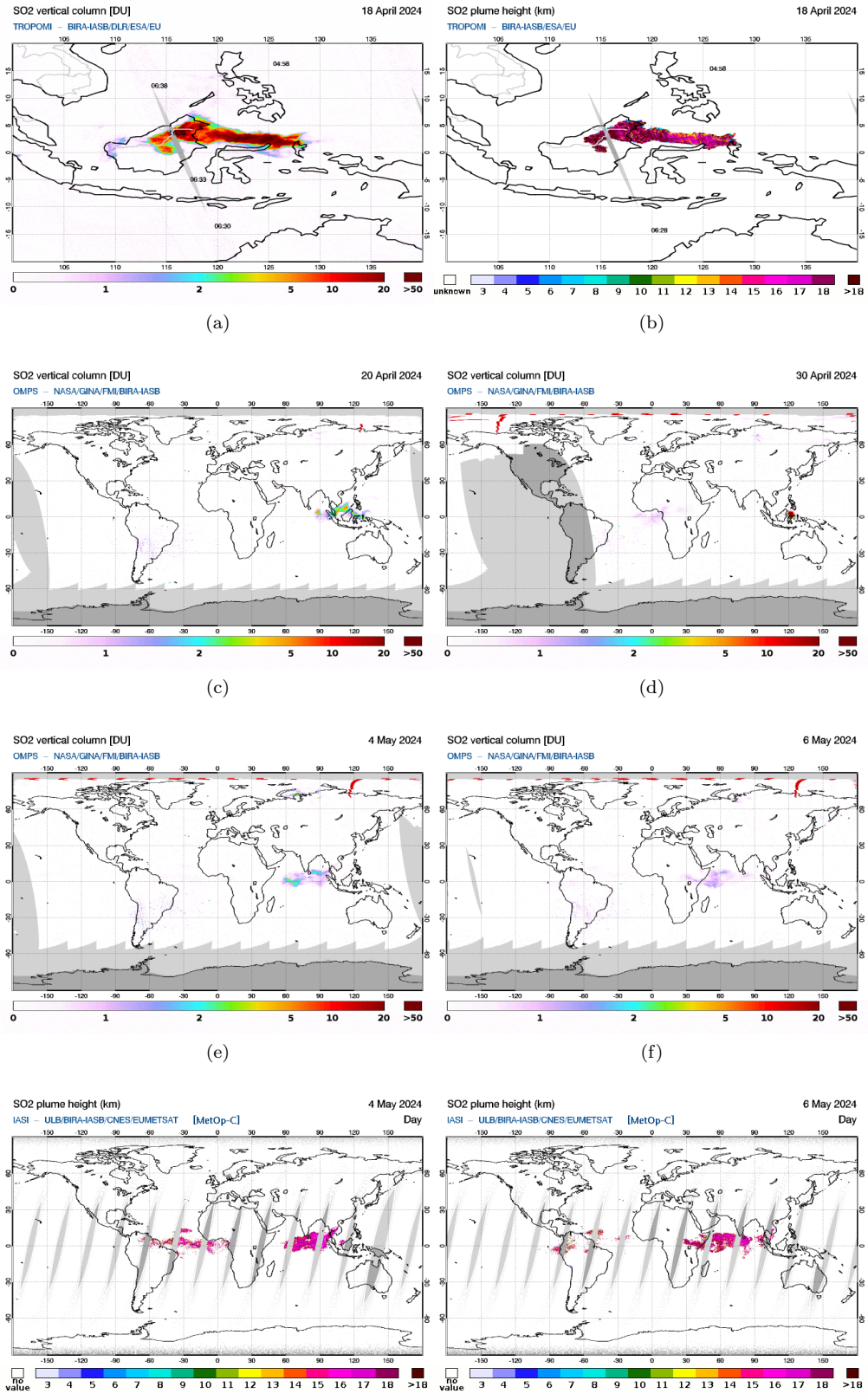

Figure 1: Ruang eruption observed by TROPOMI, OMPS, and IASI using SO_2 vertical column densities and plume height. All Images are from SACS [19]. Gray areas are the regions that were not covered by the satellite on that particular day. a) SO_2 vertical column density observed on 18 April 2024 from TROPOMI. b) SO_2 plume height observed on 18 April 2024 from TROPOMI. c) SO_2 vertical column density observed on 20 April 2024 from OMPS. d) SO_2 vertical column density observed on 30 April 2024 from OMPS. e) SO_2 vertical column density observed on 4 May 2024 from OMPS. f) SO_2 vertical column density observed on 6 May 2024 from OMPS. g) SO_2 plume height observed on 4 May 2024 from IASI. h) SO_2 plume height observed on 6 May 2024 from IASI.

The transmittance spectra obtained from the Atmospheric Chemistry Experiment (ACE) yield insights into the composition of gas phase molecules, aerosols, and clouds [27, 28]. The data on SO_2 volume mixing ratios (VMRs) and aerosol extinction provided by ACE offer significant potential for monitoring volcanic eruptions [29]. ACE utilizes the solar occultation technique, which offers high sensitivity. ACE measurements from a volcanic eruption can be used to validate other SO_2 data products, such as those from the Microwave Limb Sounder (MLS) [30]. By combining infrared aerosol transmittance spectra from the ACE-FTS with visible and near-infrared extinction data from coincident SAGE III/ISS measurements, Boone et al. [31] have derived the properties of stratospheric sulfate aerosols, **demonstrating the potential** of this combined approach to better characterize sulfate aerosols. The residual ACE spectra also enable a comprehensive characterization of sulfate aerosols resulting from volcanic eruptions [32, 33]. This study focuses on analyzing the ACE data related to the Ruang volcanic eruption that occurred in April 2024.

2. ACE measurements and location

The ACE (Atmospheric Chemistry Experiment), also known as SCISAT, is a Canadian satellite mission collecting data since February 2004 to study Earth's atmosphere. It uses solar occultation measurements to gather data and has the ACE-FTS (Atmospheric Chemistry Experiment Fourier Transform Spectrometer) as its main instrument, which provides high-resolution and broad spectral coverage (750 to 4400 cm^{-1}). The ACE-FTS is equipped with two filtered solar imagers around 0.525 μm (VIS - visible) and 1.02 μm (NIR - near-infrared) to measure atmospheric extinction. Details on the ACE mission and instruments are provided in Bernath et al. [34] and Bernath [27]. VMRs of gas phase molecules such as SO_2 are derived from ACE-FTS measurements, while aerosol extinction profiles are obtained using near-infrared (NIR) imager data.

Daily ACE sunrise measurements were on a latitude circle near 80°S at the beginning of April and moved northwards during April 2024, crossing the equator on April 26. The SO_2 plume observed by TROPOMI on April 18, 2024, is shown in Figs. 1a and 1b, while ACE was measuring near 60°S. After April 24, 2024, the ACE measurements moved towards the equator. For instance, the locations of ACE on April 27, 2024, are depicted in Fig. 2 along with the height of the SO_2 plume observed by the IASI aboard the MetOp-C satellite on April 27, 2024, provided by SACS [19]. Towards the end of April, ACE captured the plume from the Ruang eruption, as evident from Fig. 2.

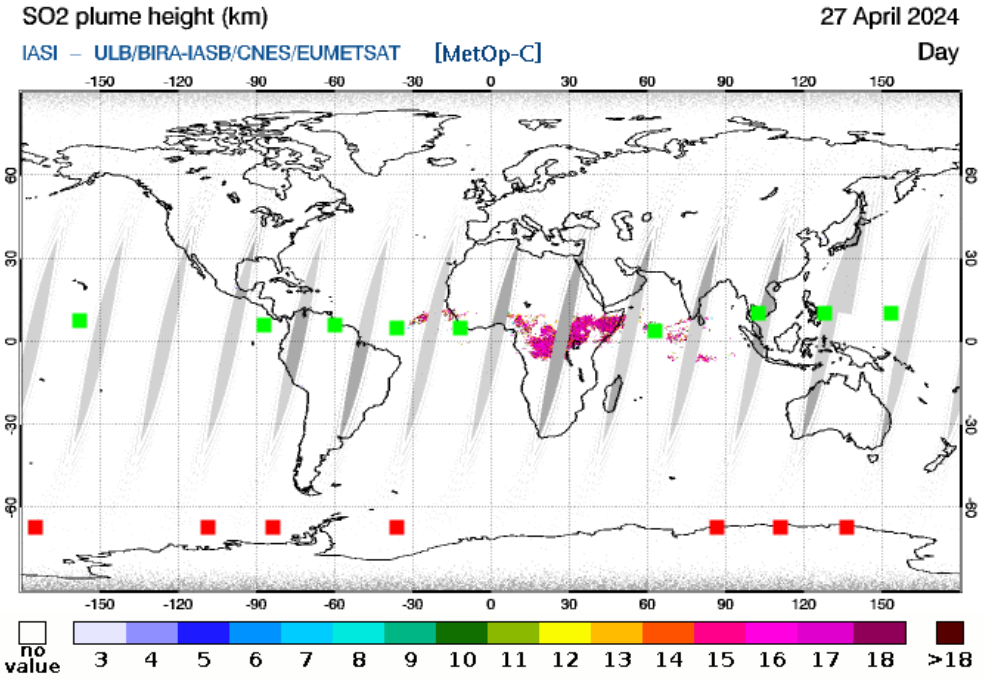

Figure 2: SO_2 plume height observed by IASI [C] on 27 April 2024 (Data is from SACS [19]). The ACE measurement locations on 27 April 2024 are shown in squares. Sunrise measurements are in green, and red squares mark sunset measurements.

The near global coverage provided by the ACE measurements allows background levels of gas phase molecules and aerosols to be determined, thus allowing volcanic eruptions to be identified in the data. The transmission spectra measured by ACE-FTS are analyzed on the ground to provide VMRs for atmospheric gases [27]. The residual spectra, obtained by removing the absorption features of gaseous molecules, contain broad features attributed to clouds and aerosol particles [33, 35]. Simulating these characteristic spectra can **yield information** on particle composition, particle size, and shape [36]. ACE infrared transmission spectra of aerosols uniquely provide composition information from absorption features in contrast to optical light scattering such as measured by SAGE III/ISS. Characterization of sulfate aerosols from ACE spectra following a volcanic eruption is detailed in Boone et al. [32] and Bernath et al. [33].

3. SO_2 emissions

SO_2 VMRs are a routine data product of ACE-FTS version 5.2 processing [37]. ACE SO_2 data from volcanic eruptions have been previously published [29, 38]. **Additionally, Höpfner et al. [39] compared SO_2 measurements from MIPAS and ACE. MIPAS measurements had some biases relative to ACE. After MIPAS corrected these biases, there was good agreement with ACE and with in situ aircraft measurements.**

To determine the altitude of the plume due to the Ruang volcanic eruption, SO_2 VMRs from

ACE-FTS in the month of April 2024 were organized into 5° latitude bins at each altitude level on a 1 km grid. Initially, outliers, missing data (indicated by -999 in the VMR column), and scaled/extrapolated data (indicated by -888 in the VMR error column) were filtered out [40]. VMR values ranging from -200 to 6000 ppt were selected to remove any artifacts created by very large or small values. Negative VMR values may occur as an artifact of the retrieval process, primarily due to measurement noise in regions where SO_2 concentrations are extremely low. The median absolute deviation (MAD) is less sensitive to physically unrealistic values; therefore, the MAD from the median at each altitude was calculated, and any values smaller than 6 MADs were considered background SO_2 as illustrated in Fig. 3a. **The average VMR values in April are illustrated in Fig. 3b. SO_2 emitted from the volcanic eruption was identified by its significantly higher values compared to the background. There is a visible SO_2 plume between 20 - 25 km in Fig. 3b due to the Ruang volcanic eruption, identifiable by its significantly higher values compared with the background.**

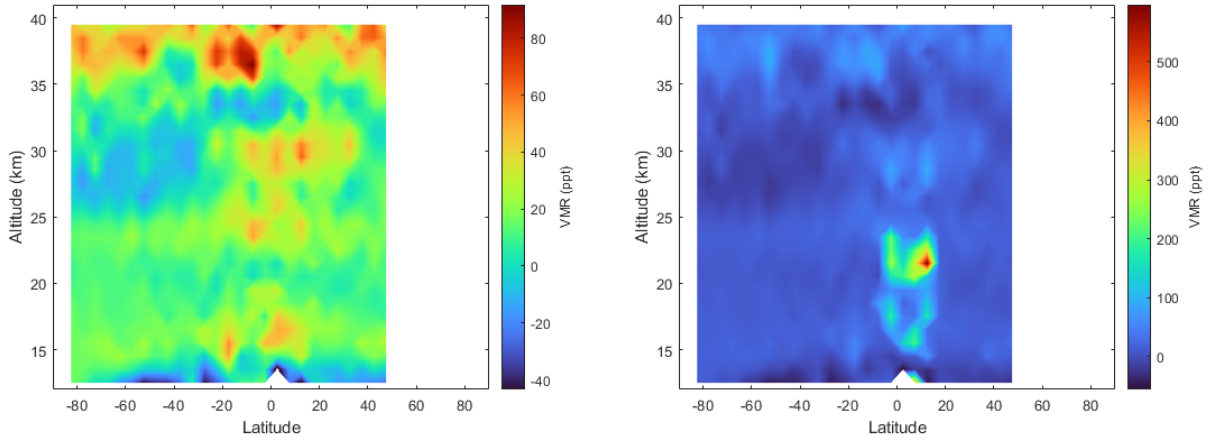

Figure 3: Global distribution of SO_2 from ACE-FTS data in April 2024. The color scale indicates VMR values in ppt. a) The background SO_2 distribution. b) SO_2 plume from the Ruang eruption.

Some individual SO_2 profiles measured by the ACE-FTS before and after the eruption are displayed in Fig. 4. There was a noticeable increase in SO_2 VMRs after the eruption at around 18 - 22 km in altitude (Fig. 4c and 4d). **The large negative values in Fig. 4 are artifacts and can be ignored. The are the result of the ACE profile retrieval of an SO_2 cloud that is localized and inhomogeneous along the line-of-sight.** During April 2024, ACE sunrise measurements are moving northward, and by May 2 measurements are at 30°N**, and elevated SO_2 values are no longer observed.** The SO_2 plume observed by IASI on April 27, 2024, overlaps with two ACE measurements (Fig. 2), and the VMR profiles are shown in Fig. 4c. The ACE profile indicates that the peak SO_2 VMR is about 4000 ppt and is around 22 km in altitude. Note that the ACE retrievals allow negative VMRs to avoid bias for low VMR values. **For retrievals with small VMRs and relatively large error bars such as SO_2 outside of volcanic plumes, forcing small VMRs to be positive introduces a positive VMR bias.**

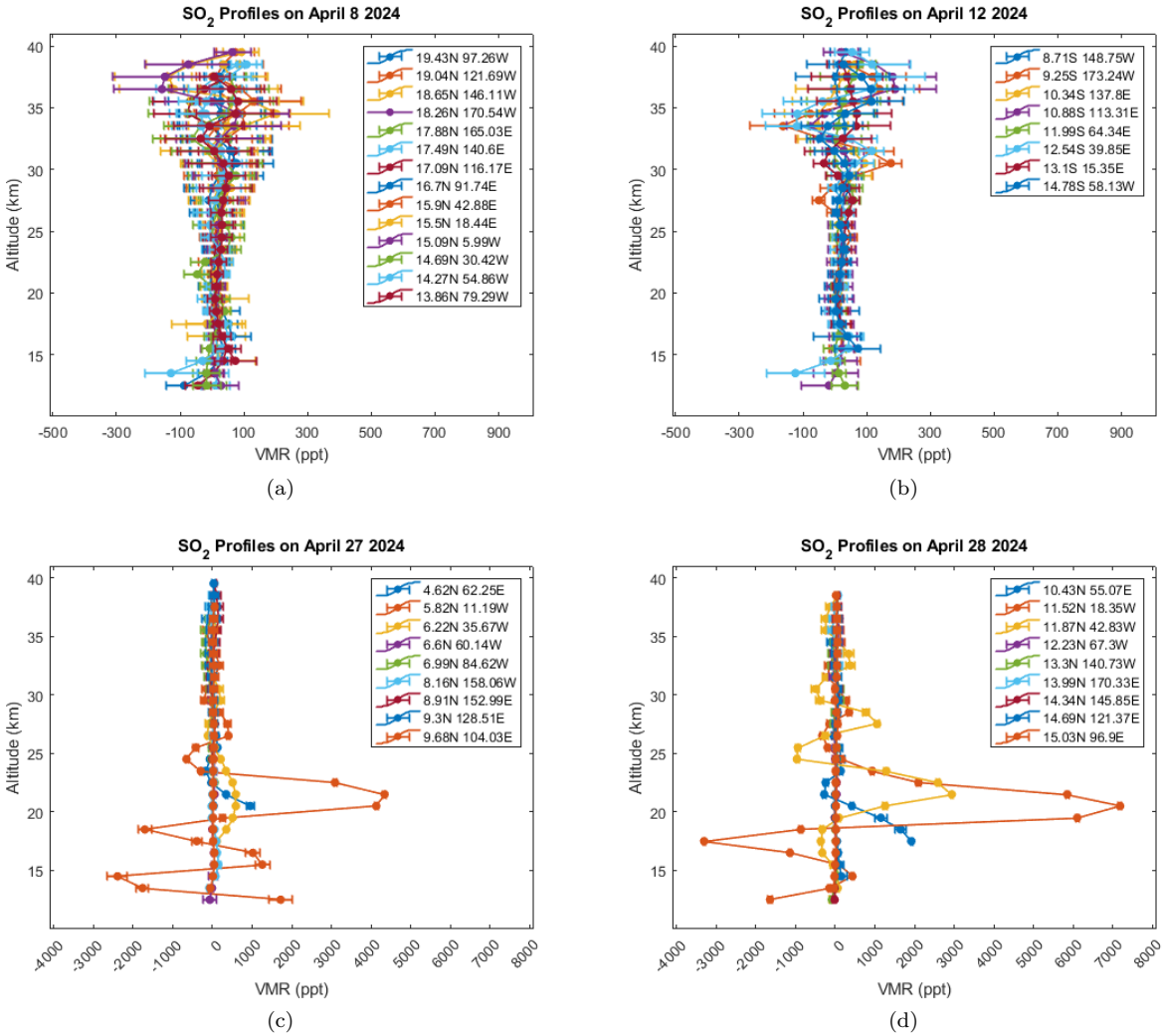

Figure 4: SO_2 VMR profiles measured in the tropical latitudes from ACE-FTS. a) Profiles measured on 08 April 2024. b) Profiles measured on 12 April 2024. c) Profiles measured on 27 April 2024. d) Profiles measured on 28 April 2024.

4. Aerosol extinction from ACE imager

Using the NIR imager on ACE-FTS, atmospheric extinction measurements were taken at 1.02 μm. Data were used from January 2024 through 13 April 2024 and 14 April through 30 April 2024. The former period is treated as background prior to the eruption. The aerosol extinctions were separated into 5° latitude and 1 km altitude bins. Fig 5 illustrates the calculated average value of the bins after excluding tropospheric clouds. The periods before and after the eruption show similar aerosol extinctions outside of the tropical region. Aerosol extinction for April and August 2022, as plotted by Bernath et al. [33] following the Hunga eruption, illustrates how aerosols were injected into the stratosphere and subsequently transported to lower altitudes in the Southern Hemisphere. Raymond et al. [4] also show sulfate aerosols following the Hunga eruption extend to southern latitudes and in early 2023 spreading through Antarctica. The persistence of the aerosol extinction pattern observed in Bernath et al. [33] and Raymond et al. [4], in Fig. 5, suggests that the elevated aerosol levels at lower altitudes in the Southern Hemisphere are likely due to sulfate aerosols from

the 2022 Hunga eruption. Boichu et al. [41] further demonstrates that volcanic aerosols remained visible in the Southern Hemisphere until May 2023, over a year after the eruption. Enhanced water vapor caused the rapid conversion of SO_2 into sulfate aerosols [42, 43, 44] and sulfate aerosols can persist for years in the stratosphere. The latter period, post Ruang eruption, displays a similar pattern but additionally there was an increase near 0° latitude from 18 km up to 22 km, as seen in Fig. 5b, **consistent with the regions of elevated SO_2 shown in Fig. 3b.** This shows the plume of the Ruang eruption rising in altitude up to around 22 km.

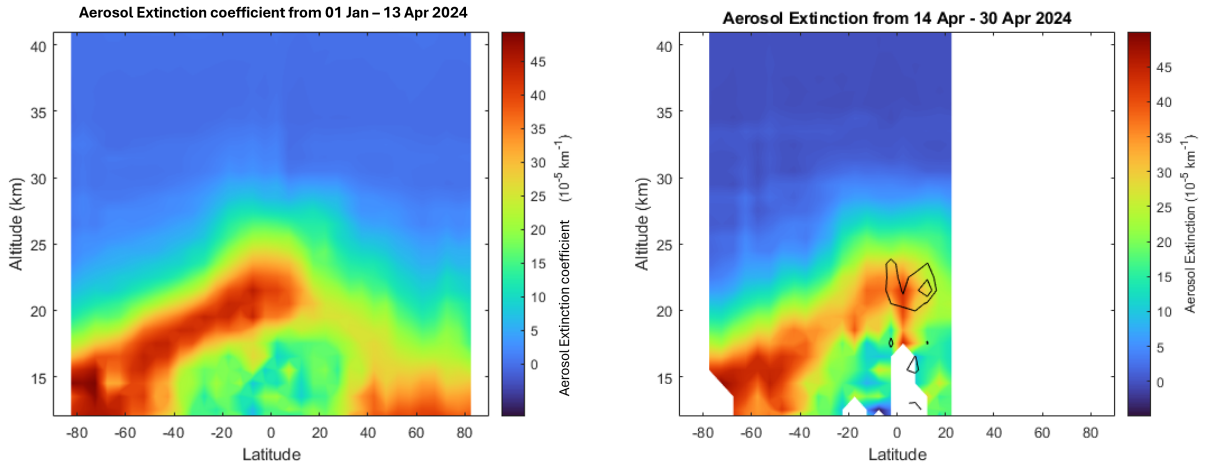

(a) (b)

Figure 5: Aerosol extinction measured by ACE-FTS NIR imager. a) Measurements from January to 13 April 2024. b) Measurements from 14 April through 30 April 2024. Elevated SO_2 indicated in Fig. 3b are shown as black contour lines.

5. Sulfate aerosols and ash

The increased levels of SO_2 (Section 3) and aerosols (Section 4) suggest the presence of stratospheric sulfate aerosols. Analyzing the ACE-FTS residual spectra offers insights into the type, size, and composition of the aerosols [32, 33]. The process for calculating the sulfate aerosol extinction spectra is described in Boone et al. [32] and Bernath et al. [33]. Essentially, sulfate aerosols are modeled as spherical liquid droplet mixtures of H_2SO_4 and H_2O. The simulated transmission spectra were determined using the Beer-Lambert law: $\tau = Ae^{-\alpha l}$, in which l (cm) represents the path length, α (cm^{-1}) is the extinction coefficient calculated assuming Mie scattering, and A is an arbitrary baseline parameter adjusted to better match the ACE spectra. The extinction coefficient as a function of wavenumber was computed using the optical constants provided by Lund Myhre et al. [45]. A mono-modal lognormal distribution was assumed [32, 33] with the geometric width parameter S fixed to 1.6. The observed residual spectra (753-4234 cm^{-1} at 2 cm^{-1} point spacing) were fitted by adjusting the parameters: median radius (r_m), A, the composition (wt% H_2SO_4), and slant column density (Nl), where N is the particle density. The path length through the aerosol plume is unknown; hence, only the column density (Nl) can be determined. The temperatures were fixed to the values from ACE-FTS version 5.2 retrievals.

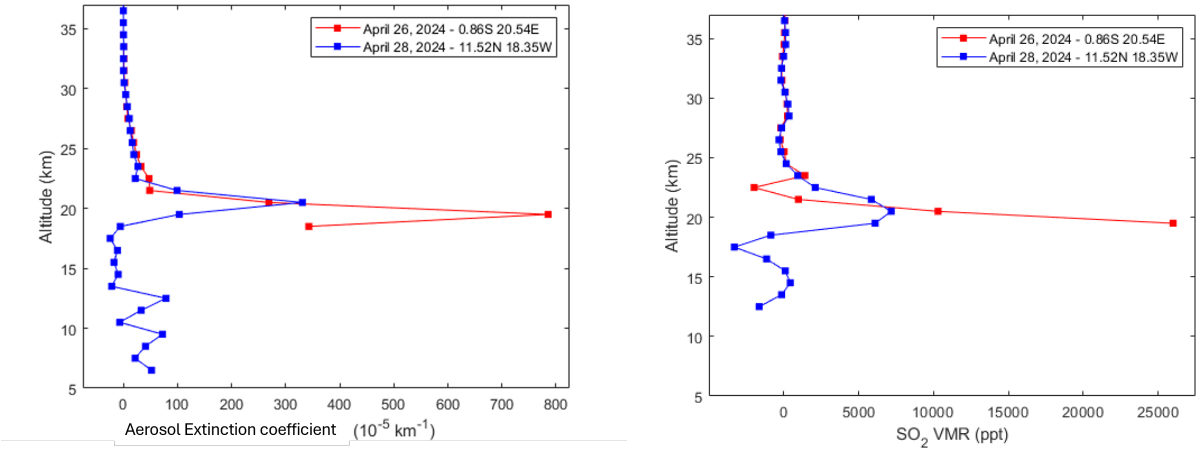

(a) (b)

Figure 6: Aerosol extinction coefficient profiles from ACE NIR imager and SO_2 VMR profiles from ACE-FTS. a) Aerosol extinction coefficient profiles from sr111575 (red) taken on April 26, 2024 at 0.86°S, 20.54°E and sr111607 (blue) taken on April 28, 2024 at 11.52°N, 18.35°W. b) SO_2 VMR profiles from the same sr111575 (red) and sr111607 (blue) occultations.

Individual aerosol extinction coefficient profiles during April between 15°S and 15°N were studied. Most of the occultations after the eruption of Ruang have background sulfate aerosols from the Hunga eruption at similar levels to the measurements before the eruption. The median radii calculated from the April 8 - 12 measurements vary from 0.05 - 0.25 μm. For example, the fitted median radius and the sulfuric acid composition for a Hunga-influenced background sulfate from April 9, 2024 (ss111336 at 20.4 km) are 0.206 μm and 65%, respectively. Some measurements capture the Ruang plume after the eruption (Table 1), and these occultations are analyzed in detail. The average particle size and composition of the Ruang aerosol plume are similar to those for the Hunga sulfate aerosols. Occultations sr111575 and sr111607 were recorded two days apart, April 26 and 28, 2024. The enhanced aerosol extinction coefficients and the SO_2 VMR profiles for these occultations can be seen in Fig. 6.

Fig. 7 displays the results for measurements at a tangent height of 20 km, where the occultations sr111575 and sr111607 show a distinct peak. The presence of sulfate aerosols is evident, as the calibrated measurements **(Observed spectra shown in blue in Fig. 7a and 7c)** are reproduced by the fitted spectra, except for mainly two regions near 1000 cm^{-1} and 1400 cm^{-1}.

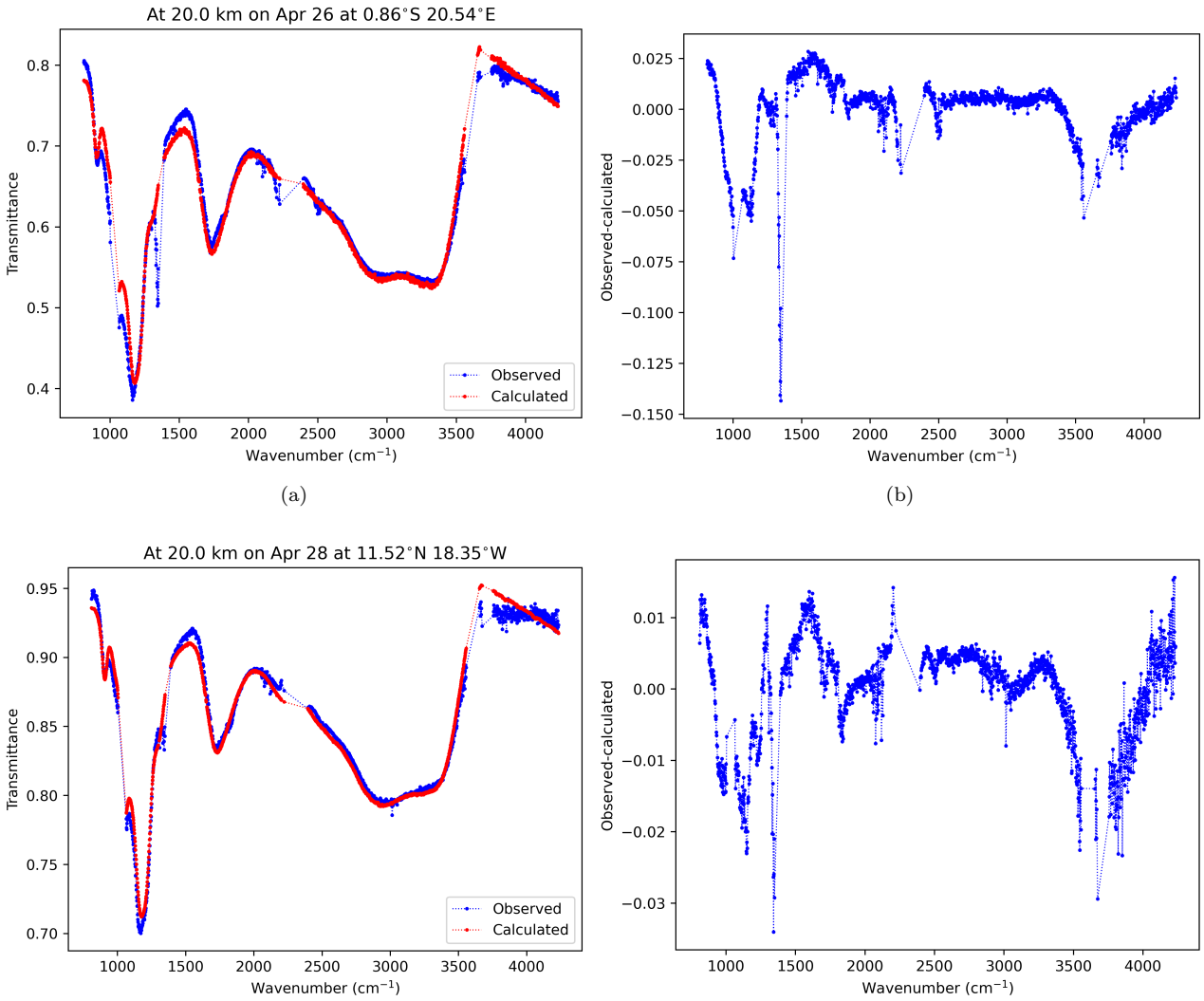

Figure 7: a) The observed (blue) and calculated (red) spectra for the occultation on April 26 at 0.86°S, 20.54°E (sr111575) at a tangent altitude of 20 km. b) The residual (observed-calculated) values for the occultation sr111575. c) The observed (blue) and calculated (red) spectra for the occultation on April 28, 2024 at 11.52°N, 18.35°W (sr111607) at a tangent altitude of 20 km. d) The residual (observed-calculated) values for the occultation sr111607.

Parameters in Table 1 were used to calculate the spectra shown in red in Figs. 7a and 7c. The path length across the limb is unknown; therefore, the slant column density (Nl) in particles/cm^2 is calculated. These findings indicate that the sulfate aerosols in the plume near 20 km contain approximately 65% sulfuric acid. Bernath et al. [33] characterize the stratospheric sulfate aerosols released from the Hunga volcano providing wt% H_2SO_4 ranging from 50% to 80% depending on the atmospheric temperature. Boone et al. [31] combining ACE-FTS and SAGE III/ISS measurements indicate sulfuric acid levels ranging from 65.6% - 73.8% for the 2019 Raikoke eruption and 68.4% - 74.3% for the Hunga eruption. Boone et al. [32] show a blanket of sulfate aerosols ranging from the tropopause to 20 km over northern latitudes for many months, and the sulfuric acid composition was as low as 53%. Although many sulfate aerosol studies conventionally fix the sulfuric acid content at 75% for simplicity, these findings highlight that the actual content can vary depending on atmospheric conditions [31]. The observed - calculated plots (in blue Figs. 7b and 7d) show

3 regions of interest. Near 3500 cm^{-1}, the model has problems reproducing the observations. The sharp feature at about 1400 cm^{-1} is an artifact from the strong SO_2 lines that are not simulated properly in calculating the experimental residual spectrum (in red on the left). The wide feature near 1000 cm^{-1} is from silicate in volcanic ash [35]. Minimizing the residuals around 1000 cm^{-1} to account for the missing ash contribution in that spectral region results in a slight mismatch between the measured and fitted spectra near 3500 cm^{-1}, introducing a systematic feature in the residuals. In addition to the two occultations shown in Fig. 7, other occultations were also fitted, and the results are provided in Table 1. Occultations sr111575 and sr111607 are the only two that show spectral features due to volcanic ash in addition to sulfate aerosol features. Ash particles are relatively large and settle quickly out of the stratosphere. The transmittance spectrum indicating sulfate aerosols without ash from the Ruang plume is illustrated in Fig. 8 along with the residual spectra. The calculated sulfate aerosol spectra agree well with the observed spectra as evident by Fig. 8. Calculated sulfate aerosol spectra agree with the observed spectra in each of the occultations in Table 1 at the given tangent altitudes.

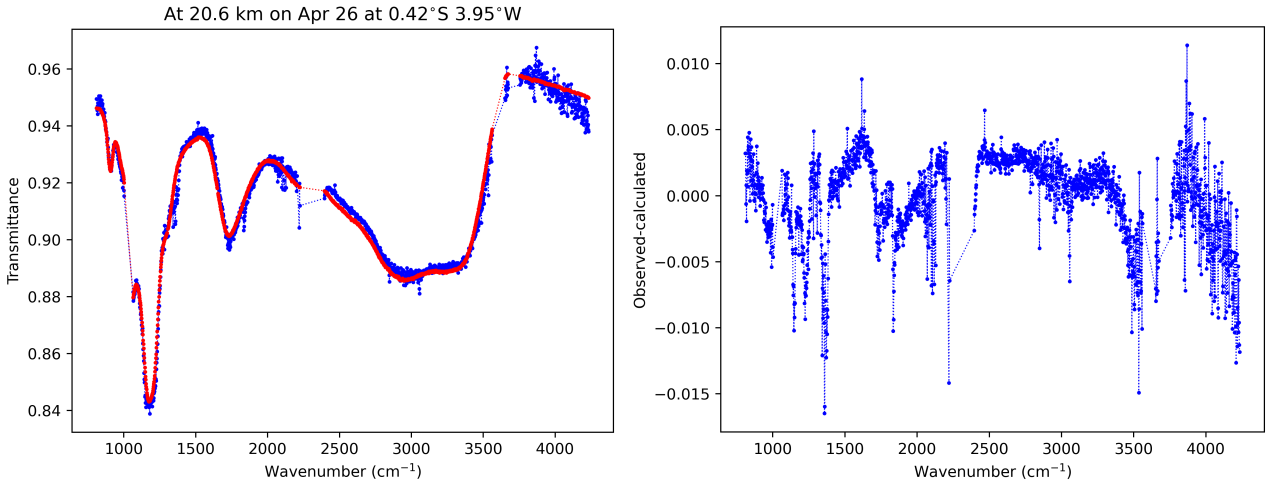

(a) (b)

Figure 8: a) The observed (blue) and calculated (red) spectra for the occultation on April 26 at 0.42°S, 3.95°E (sr111576) at a tangent altitude of 20.6 km. b) The residual (observed-calculated) values for the occultation sr111576.

Table 1: Fitting results for some selected occultations. The complete fitted result for each occultation is provided in the supplementary files.

Occultation	Location	Date	Tangent height (km)	wt% H_2SO_4	Median radius (μm)	Temperature (K)	column density ($\times 10^8$ particles/cm^2)
sr111575	0.86°S 20.54°E	Apr 26	20.0	63.96 ± 0.11	0.145 ± 0.001	199.8	22.66 ± 0.47
sr111575	0.86°S 20.54°E	Apr 26	21.2	64.31 ± 0.19	0.152 ± 0.002	203.6	8.441 ± 0.32
sr111576	0.42°S 3.95°W	Apr 26	20.6	65.00 ± 0.33	0.124 ± 0.005	197.1	6.83 ± 0.84
sr111576	0.42°S 3.95°W	Apr 26	21.5	66.47 ± 0.31	0.106 ± 0.006	200.4	9.9 ± 1.3
sr111577	0.01°N 28.43°W	Apr 26	21.7	66.07 ± 0.43	0.196 ± 0.005	205.1	1.179 ± 0.091
sr111584	2.97°N 160.18°E	Apr 26	20.5	70.55 ± 0.93	0.167 ± 0.011	205.1	0.99 ± 0.20
sr111607	11.52°N 18.35W	Apr 28	20.0	65.56 ± 0.15	0.156 ± 0.002	197.9	7.77 ± 0.30
sr111608	11.87°N 42.83°W	Apr 28	19.0	67.96 ± 0.52	0.085 ± 0.011	197.0	11.7 ± 4.0
sr111608	11.87°N 42.83°W	Apr 28	21.0	68.80 ± 0.36	0.098 ± 0.006	204.0	12.1 ± 1.9
sr112218	24.47°N 58.58°E	Jun 8	19.4	64.85 ± 0.24	0.124 ± 0.003	195.0	9.48 ± 0.62
sr112218	24.47°N 58.58°E	Jun 8	19.9	66.02 ± 0.24	0.131 ± 0.004	198.8	7.55 ± 0.60
sr112218	24.47°N 58.58°E	Jun 8	20.1	66.79 ± 0.24	0.117 ± 0.004	200.5	9.78 ± 0.90
sr112218	24.47°N 58.58°E	Jun 8	2 0.5	67.88 ± 0.32	0.113 ± 0.005	204.4	9.4 ± 1.1
sr112231	12.46°N 72.78°E	Jun 9	18.9	63.00 ± 0.24	0.134 ± 0.003	195.6	7.84 ± 0.48
sr112231	12.46°N 72.78°E	Jun 9	19.2	62.59 ± 0.24	0.113 ± 0.003	195.8	12.85 ± 0.87
sr112231	12.46°N 72.78°E	Jun 9	19.4	63.48 ± 0.25	0.121 ± 0.003	196.2	10.29 ± 0.70
sr112231	12.46°N 72.78°E	Jun 9	19.8	64.50 ± 0.28	0.108 ± 0.004	197.1	13.2 ± 1.2
sr112231	12.46°N 72.78°E	Jun 9	20.0	65.00 ± 0.25	0.124 ± 0.004	198.3	8.66 ± 0.79
sr112231	12.46°N 72.78°E	Jun 9	20.3	65.27 ± 0.26	0.096 ± 0.005	199.9	15.7 ± 2.0
sr112231	12.46°N 72.78°E	Jun 9	20.6	66.68 ± 0.27	0.135 ± 0.004	201.9	5.46 ± 0.48

The occultations detailed in Table 1 indicate that ACE captured the plume from the Ruang eruption

in tropical latitudes at the end of April and early June. The sulfate aerosol spectra calculated from all the occultations given in Table 1 show H_2SO_4 content by weight ranging from 62.59% to 70.55%, with an average of 64%. The median radius of the sulfate aerosols varies from 0.085 μm to 0.196 μm, averaging 0.127 μm. The sulfate aerosols released from the Hunga volcano had an average median radius of 0.297 $\pm$ 0.002 μm and an average H_2SO_4 content of 70.4% [33]. Balloon-borne characterization of the Hunga plume a week after the eruption by Kloss et al. [46] reports predominant sulfate aerosol particles with sizes between 0.5 - 1 μm and small sulfate particles with sizes below 0.5 μm.

The expected H_2SO_4 content of a volcanic plume for a given temperature and ambient H_2O vapor pressure can be calculated from the model provided by Bernath et al. [33], which was derived using the data from the Hunga and Raikoke eruptions. The calculated wt% H_2SO_4 for the occultations sr111575 (April 26), sr111576 (April 26), sr111608 (April 28), sr112218 (June 8), and sr112231 (June 9) along with the sulfuric content obtained from the fitting (Table 1) is illustrated in Fig. 9a. The estimated H_2SO_4 content from the formula has an uncertainty of 5%. Water vapor pressure is calculated from ACE-FTS retrievals. Fig. 9b illustrates the temperature dependence of the fitted wt% H_2SO_4 provided in Table 1. As shown in Fig. 9b, the wt% of H_2SO_4 increases with temperature, which occurs as water evaporates from the aerosols with rising temperatures.

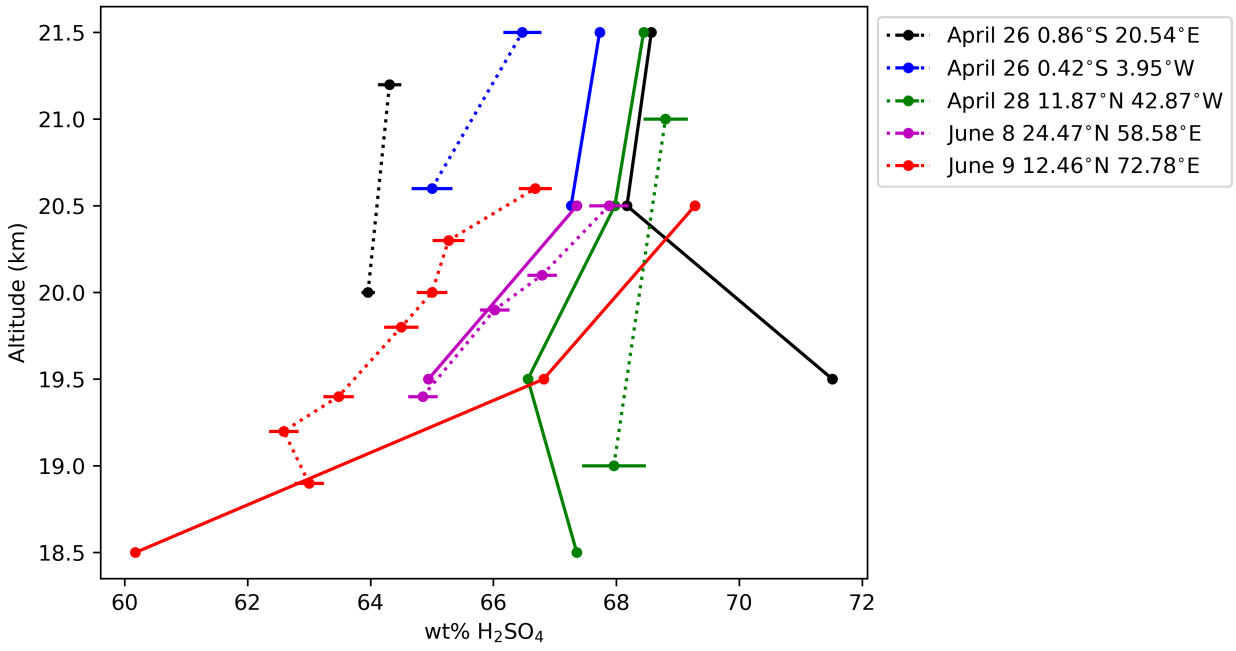

(a)

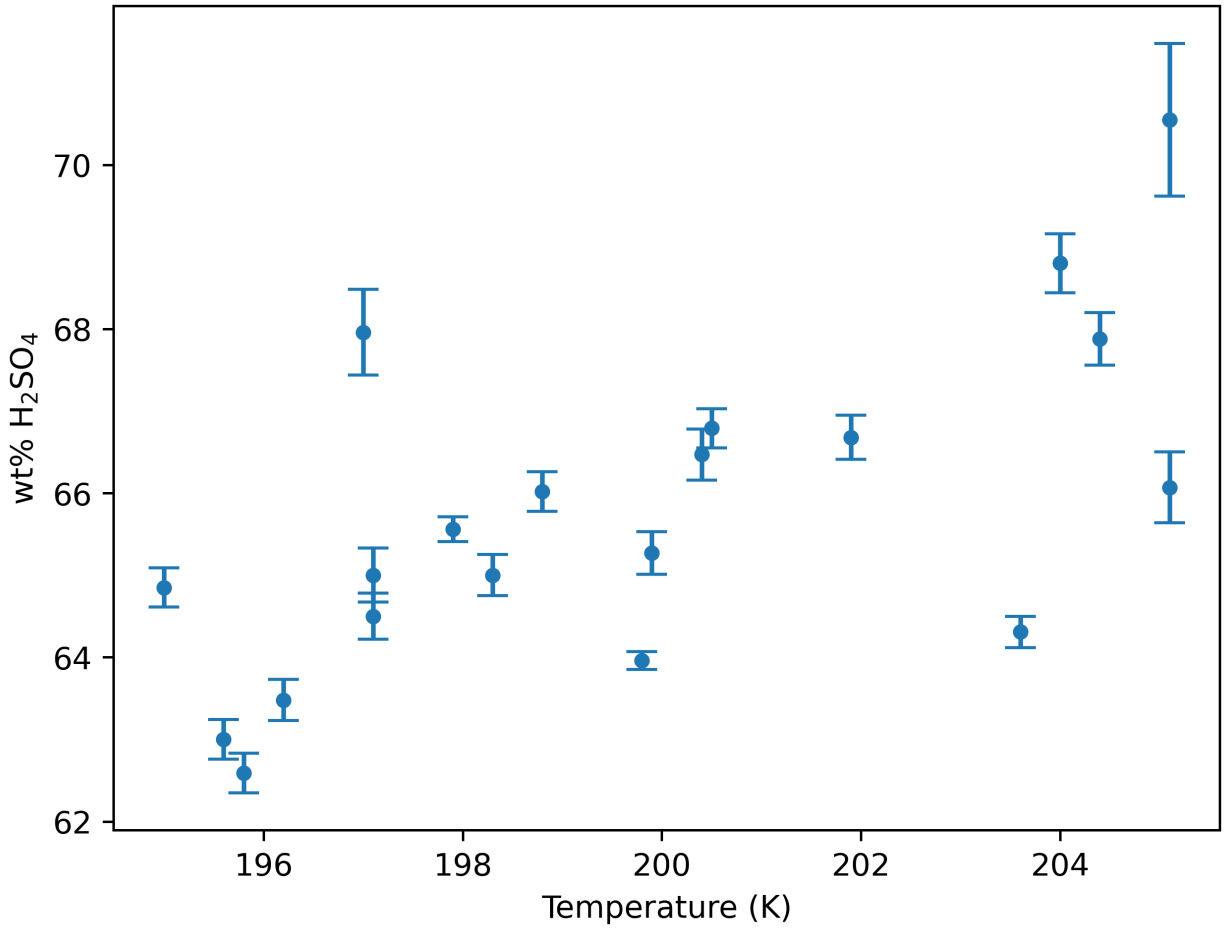

(b)

Figure 9: a) wt% H_2SO_4 as a function of altitude for selected occultations. Solid lines represent the calculations from the empirical formula given in Bernath et al. [33]. Dashed lines represent the values taken from Table 1. b) wt% H_2SO_4 obtained from the fitted results as a function of temperature.

The effective radius was calculated using a monomodal distribution, as outlined by Boone et al. [31] using equation (4) in that paper, to compare with the observed sulfate aerosol sizes from various volcanic events. The monomodal fitting results for the Ruang, Raikoke, and **Hunga** eruptions, as well as background sulfate aerosols, are illustrated in Fig. 10. **The effective radii calculated for the Raikoke eruption fall within the values derived from SAGE III measurements by Wrana et al. [47] and Khaykin et al. [48] report a maximum effective radius of 0.4 μm for Hunga eruption from April 2022 SAGE III measurements.** The effective radii calculated for Ruang in April show significant scatter, suggesting high variability in particle size shortly after the eruption. By June, aerosols above 17 km are similar in size to those observed after the Raikoke eruption, which were taken 3-10 months post-eruption. The aerosol size from the Ruang eruption is larger than the background levels but significantly smaller than those from the **Hunga** eruption.

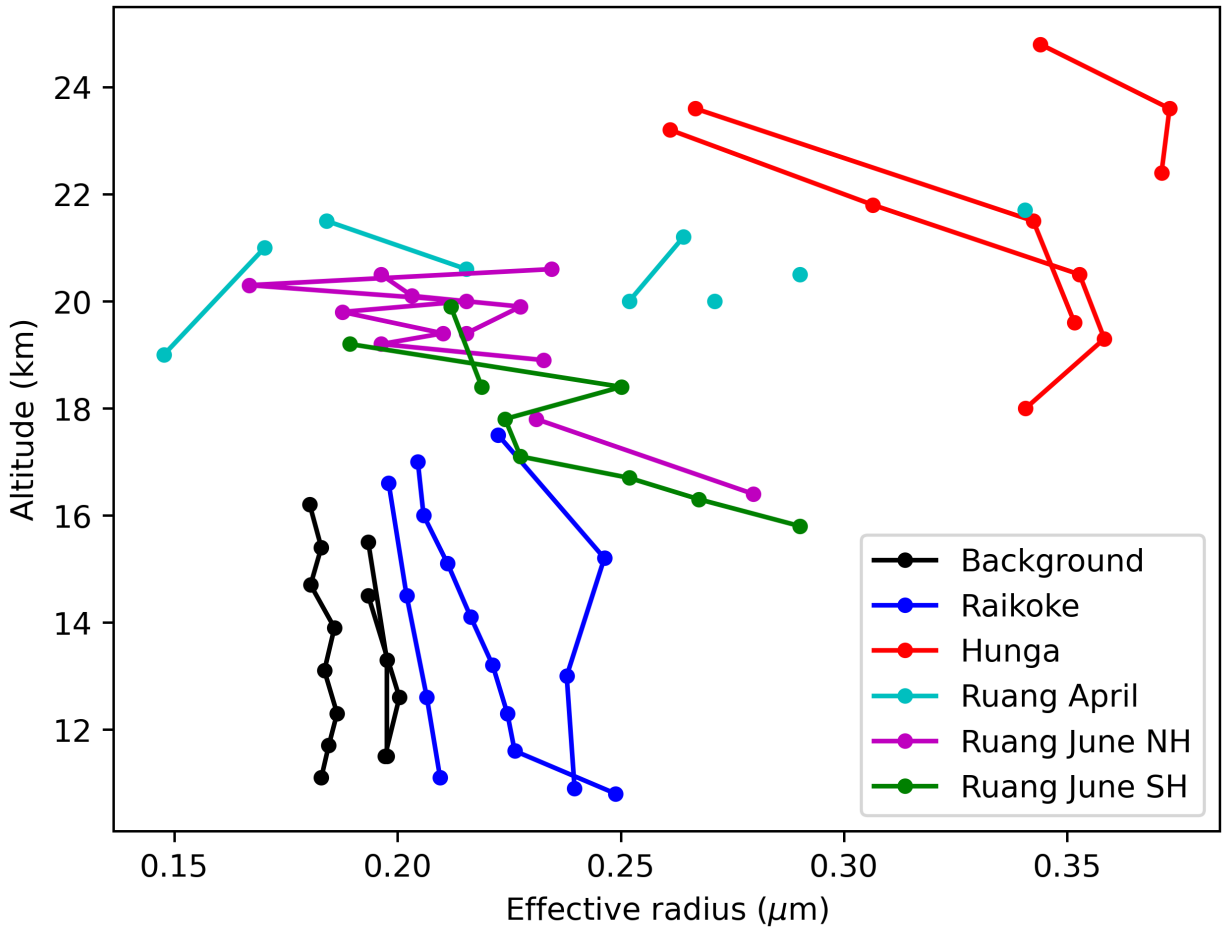

Figure 10: Effective radius profiles using monomodal distribution. The results for the Ruang are calculated from the fitting results shown in Table 1. The background, Raikoke, and Hunga results are from Boone et al. [31]

6. Conclusion

ACE was conducting measurements in southern latitudes when the Ruang volcano erupted on April 16, 2024. Later in that month, it captured the plume from the eruption. ACE measured enhanced SO_2 correlated with

sulfate aerosol extinction at approximately 20 km altitude, extending west of the volcano after the initial event. The observed aerosols were identified as stratospheric sulfate aerosols using the ACE residual spectra, which also showed silicate features from volcanic ash in two occultations. The average size of the observed sulfate aerosols is 0.127 μm, with 64% of H_2SO_4 content by weight. The observed sulfate aerosols are similar in size to the ones observed from the Raikoke eruption and smaller than the **Hunga** eruption. Data from the ACE-FTS and the 1-micron imager prove valuable in observing and characterizing volcanic eruptions.

7. Acknowledgments

The ACE mission is funded by the Canadian Space Agency. Some support was also provided by NASA through the SAGE-III-ISS Science Team (80NSSC21K1194). PB acknowledges RB for productive discussion.

References

[1] Cole-Dai J. Volcanoes and climate. Wiley Interdisciplinary Reviews: Climate Change 2010;1(6):824–839. doi:10.1002/wcc.76.

[2] Millan L, Santee ML, Lambert A, Livesey NJ, Werner F, Schwartz MJ, et al. The Hunga Tonga-Hunga Ha'apai hydration of the stratosphere. Geophysical Research Letters 2022;49(13):e2022GL099381. doi:10.1029/2022GL099381.

[3] Vömel H, Evan S, Tully M. Water vapor injection into the stratosphere by Hunga Tonga-Hunga Ha'apai. Science 2022;377(6613):1444–1447. doi:10.1126/science.abq2.

[4] Raymond N, Bernath P, Boone C. Atmospheric effects of the Tonga volcanic sulfate aerosols. Journal of Quantitative Spectroscopy and Radiative Transfer 2024;p. 109056. doi:10.1016/j.jqsrt.2024.109056.

[5] Coffey M. Observations of the impact of volcanic activity on stratospheric chemistry. Journal of Geophysical Research: Atmospheres 1996;101(D3):6767–6780. doi:10.1029/95JD03763.

[6] von Glasow R, Bobrowski N, Kern C. The effects of volcanic eruptions on atmospheric chemistry. Chemical Geology 2009;263(1-4):131–142. doi:10.1016/j.chemgeo.2008.08.020.

[7] Kilian M, Brinkop S, Jöckel P. Impact of the eruption of Mt Pinatubo on the chemical composition of the stratosphere. Atmospheric Chemistry and Physics 2020;20(20):11697–11715. doi:10.5194/acp-20-11697-2020.

[8] PARKER DE, Wilson H, Jones PD, Christy J, Folland CK. The impact of Mount Pinatubo on worldwide temperatures. International Journal of Climatology: A Journal of the Royal Meteorological Society 1996;16(5):487–497. doi:10.1002/(SICI)1097-0088(199605)16:5%3C487::AID-JOC39%3E3.0.CO;2-J.

[9] Soden BJ, Wetherald RT, Stenchikov GL, Robock A. Global cooling after the eruption of Mount Pinatubo: A test of climate feedback by water vapor. science 2002;296(5568):727–730. doi:10.1126/science.296.5568.727.

[10] Thompson DW, Wallace JM, Jones PD, Kennedy JJ. Identifying signatures of natural climate variability in time series of global-mean surface temperature: Methodology and insights. Journal of Climate 2009;22(22):6120–6141. doi:10.1175/2009JCLI3089.1.

[11] Gleason J, Bhartia PK, Herman JRe, McPeters R, Newman P, Stolarski R, et al. Record low global ozone in 1992. Science 1993;260(5107):523–526. doi:10.1126/science.260.5107.523.

[12] Randel WJ, Wu F, Russell III J, Waters J, Froidevaux L. Ozone and temperature changes in the stratosphere following the eruption of Mount Pinatubo. Journal of Geophysical Research: Atmospheres 1995;100(D8):16753–16764. doi:10.1029/95JD01001.

[13] Hidayat A, Marfai M, Hadmoko D. Eruption on Indonesia's volcanic islands: A review of potential hazards, fatalities, and management. In: IOP Conference Series: Earth and Environmental Science, vol. 485 IOP Publishing; 2020. p. 012061. doi:10.1088/1755-1315/485/1/012061.

[14] Sennert S. Global Volcanism Program, 2024. Report on Ruang (Indonesia). Weekly Volcanic Activity Report, 10 April-16 April 2024. Smithsonian Institution and US Geological Survey; 2024.

[15] BESSHO K, DATE K, HAYASHI M, IKEDA A, IMAI T, INOUE H, et al. An Introduction to Himawari-8/9—Japan's New-Generation Geostationary Meteorological Satellites. Journal of the Meteorological Society of Japan 2016;94(2):152. doi:10.2151/jmsj.2016-009.

[16] RAMMB-CIRA Satellite Library 2024 - Ruang Volcano; 2024. https://satlib.cira.colostate.edu/event/ruang-volcano/.

[17] Levelt PF, Van Den Oord GH, Dobber MR, Malkki A, Visser H, De Vries J, et al. The ozone monitoring instrument. IEEE Transactions on geoscience and remote sensing 2006;44(5):1093–1101. doi:10.1109/TGRS.2006.872333.

[18] Acker J, Sulfur dioxide (SO2) from eruption of Ruang Volcano observed by OMI and TROPOMI. NASA; 2024. https://disc.gsfc.nasa.gov/information/data-in-action?title=Sulfur+dioxide+%28SO2%29+from+eruption+of+Ruang+Volcano+observed+by+OMI+and+TROPOMI.

[19] Support to Aviation Control Service. Royal Belgian Institute for Space Aeronomy;. https://sacs.aeronomie.be/.

[20] Chan KL, Valks P, Heue KP, Lutz R, Hedelt P, Loyola D, et al. Global Ozone Monitoring Experiment-2 (GOME-2) daily and monthly level-3 products of atmospheric trace gas columns. Earth System Science Data 2023;15(4):1831–1870. doi:10.5194/essd-15-1831-2023.

[21] Veefkind JP, Aben I, McMullan K, Förster H, De Vries J, Otter G, et al. TROPOMI on the ESA Sentinel-5 Precursor: A GMES mission for global observations of the atmospheric composition for climate, air quality and ozone layer applications. Remote sensing of environment 2012;120:70–83. doi:10.1016/j.rse.2011.09.027.

[22] Flynn LE, Seftor CJ, Larsen JC, Xu P. The ozone mapping and profiler suite. In: Earth Science Satellite Remote Sensing: Vol. 1: Science and Instruments Springer; 2006.p. 279–296. doi:10.1007/978-3-540-37293-6_15.

[23] Clerbaux C, Boynard A, Clarisse L, George M, Hadji-Lazaro J, Herbin H, et al. Monitoring of atmospheric composition using the thermal infrared IASI/MetOp sounder. Atmospheric Chemistry and Physics 2009;9(16):6041–6054. doi:10.5194/acp-9-6041-2009.

[24] Aumann HH, Pagano TS, Strow LL. Atomospheric Infrared Sounder (AIRS) on the Earth Observing System. In: Hyperspectral Remote Sensing of the Land and Atmosphere, vol. 4151 SPIE; 2001. p. 115–125. doi:10.1117/12.416998.

[25] Sennert S. Global Volcanism Program, 2024. Report on Ruang (Indonesia). Weekly Volcanic Activity Report, 24 April-30 April 2024. Smithsonian Institution and US Geological Survey; 2024.

[26] Voiland A, A blanket of ash from Ruang. NASA; 2024. https://earthobservatory.nasa.gov/images/152716/a-blanket-of-ash-from-ruang#:~:text=After%20the%20eruption%20at%20Ruang,satellites%20measured%20about%200.3%20teragrams.

[27] Bernath P. The Atmospheric Chemistry Experiment (ACE). Journal of Quantitative Spectroscopy and Radiative Transfer 2017;186:3–16. doi:/10.1016/j.jqsrt.2016.04.006.

[28] Bernath P. The Atmospheric Chemistry Experiment (ACE): Aerosol and gas analysis from orbit. TrAC Trends in Analytical Chemistry 2023;p. 117207. 10.1016/j.trac.2023.117207.

[29] Cameron WD, Bernath P, Boone C. Sulfur dioxide from the atmospheric chemistry experiment (ACE) satellite. Journal of Quantitative Spectroscopy and Radiative Transfer 2021;258:107341. doi:10.1016/j.jqsrt.2020.107341.

[30] Pumphrey H, Read W, Livesey N, Yang K. Observations of volcanic SO 2 from MLS on Aura. Atmospheric Measurement Techniques 2015;8(1):195–209. doi:10.5194/amt-8-195-2015.

[31] Boone C, Bernath P, Pastorek A, Lecours M. Sulfate aerosol properties derived from combining coincident ACE-FTS and SAGE III/ISS measurements. Journal of Quantitative Spectroscopy and Radiative Transfer 2023;p. 108815. doi:10.1016/j.jqsrt.2023.108815.

[32] Boone CD, Bernath PF, Labelle K, Crouse J. Stratospheric aerosol composition observed by the Atmospheric Chemistry Experiment following the 2019 Raikoke eruption. Journal of Geophysical Research: Atmospheres 2022;127(18):e2022JD036600. doi:10.1029/2022JD036600.

[33] Bernath P, Boone C, Pastorek A, Cameron D, Lecours M. Satellite characterization of global stratospheric sulfate aerosols released by Tonga volcano. Journal of Quantitative Spectroscopy and Radiative Transfer 2023;299:108520. doi:10.1016/j.jqsrt.2023.108520.

[34] Bernath PF, McElroy CT, Abrams M, Boone CD, Butler M, Camy-Peyret C, et al. Atmospheric chemistry experiment (ACE): mission overview. Geophysical research letters 2005;32(15). doi:10.1029/2005gl022386.

[35] Lecours MJ, Bernath PF, Sorensen JJ, Boone CD, Johnson RM, LaBelle K. Atlas of ACE spectra of clouds and aerosols. Journal of Quantitative Spectroscopy and Radiative Transfer 2022;292:108361. doi:10.1016/j.jqsrt.2022.108361.

[36] Lecours M, Bernath P, Boone C, Crouse J. Infrared transmittance spectra of polar stratospheric clouds. Journal of Quantitative Spectroscopy and Radiative Transfer 2023;294:108406. doi:10.1016/j.jqsrt.2022.108361.

[37] Boone C, Bernath P, Lecours M. Version 5 retrievals for ACE-FTS and ACE-imagers. Journal of Quantitative Spectroscopy and Radiative Transfer 2023;p. 108749. doi:10.1016/j.jqsrt.2023.108749.

[38] Bernath P, Bhushal M. Sulfur dioxide sources in the stratosphere. Journal of Quantitative Spectroscopy and Radiative Transfer 2024;doi:10.1016/j.jqsrt.2024.109217.

[39] Höpfner M, Boone C, Funke B, Glatthor N, Grabowski U, Günther A, et al. Sulfur dioxide (SO 2) from MIPAS in the upper troposphere and lower stratosphere 2002–2012. Atmospheric Chemistry and Physics 2015;15(12):7017–7037. doi:10.5194/acp-15-7017-2015.

[40] Boone C, Bernath P, Data usage guide and file format description for ACE-FTS level 2 data version 5.2 ASCII format; 2022. https://databace.scisat.ca/level2/ace_v5.2/ACE-SOC-0043-ACE-FTS_ascii_data_usage_and_fileformat_for_v5.2.pdf.

[41] Boichu M, Grandin R, Blarel L, Torres B, Derimian Y, Goloub P, et al. Growth and global persistence of stratospheric sulfate aerosols from the 2022 Hunga Tonga–Hunga Ha'apai volcanic eruption. Journal of Geophysical Research: Atmospheres 2023;128(23):e2023JD039010. doi:10.1029/2023JD039010.

[42] Zhu Y, Bardeen CG, Tilmes S, Mills MJ, Wang X, Harvey VL, et al. Perturbations in stratospheric aerosol evolution due to the water-rich plume of the 2022 Hunga-Tonga eruption. Communications Earth & Environment 2022;3(1):248. doi:10.1038/s43247-022-00580-w.

[43] Legras B, Duchamp C, Sellitto P, Podglajen A, Carboni E, Siddans R, et al. The evolution and dynamics of the Hunga Tonga–Hunga Ha'apai sulfate aerosol plume in the stratosphere. Atmospheric Chemistry and Physics 2022;22(22):14957–14970. doi:10.5194/acp-22-14957-2022.

[44] Sellitto P, Podglajen A, Belhadji R, Boichu M, Carboni E, Cuesta J, et al. The unexpected radiative impact of the Hunga Tonga eruption of 15th January 2022. Communications Earth & Environment 2022;3(1):288. doi:10.1038/s43247-022-00618-z.

[45] Lund Myhre CE, Christensen DH, Nicolaisen FM, Nielsen CJ. Spectroscopic study of aqueous H2SO4 at different temperatures and compositions: Variations in dissociation and optical properties. The Journal of Physical Chemistry A 2003;107(12):1979–1991. doi:10.1021/jp026576n.

[46] Kloss C, Sellitto P, Renard JB, Baron A, Bègue N, Legras B, et al. Aerosol characterization of the stratospheric plume from the volcanic eruption at Hunga Tonga 15 January 2022. Geophysical Research Letters 2022;49(16):e2022GL099394. doi:10.1029/2022GL099394.

[47] Wrana F, Niemeier U, Thomason LW, Wallis S, von Savigny C. Stratospheric aerosol size reduction after volcanic eruptions. Atmospheric Chemistry and Physics 2023;23(17):9725–9743. doi:10.5194/acp-23-9725-2023.

[48] Khaykin S, Podglajen A, Ploeger F, Grooß JU, Tencé F, Bekki S, et al. Global perturbation of stratospheric water and aerosol burden by Hunga eruption. Communications Earth & Environment 2022;3(1):316. doi:10.1038/s43247-022-00652-x.